Development of Fe-Mn alloy coatings using Coaxial laser assisted cold spray process

By

Sathwik Reddy Toom

A dissertation submitted in partial fulfillment

of the requirement for the degree of

Masters of Science in Engineering

(Mechanical Engineering)

at University of Michigan- Dearborn

2017

Master's Thesis committee

      Professor Pravansu Mohanty, Chair

      Assistant Professor Gargi Ghosh

      Assistant Professor Tanjore V. Jayaraman

`

2017

Acknowledgement

First, I would like to thank my parents for their blessings, love and support. Words cannot be expressed to put down the care, sacrifice and countless prayers they have being doing for me. I would like to thank my advisor Dr. Pravansu Mohanty for giving me this wonderful opportunity to work at Additive Manufacturing and Process Laboratory and explore in the field of Laser Assisted Cold Spray process. He has always been a constant support through various up's and down's during my master's study. I would also like to express my gratitude to my committee members

I would not have made it this far without my friends from supporting with my decisions. I would also like to thank my past and present members of Additive Manufacturing Laboratory, My teammates Dr. Vikram Varadarajan, Ramcharan Palacode Visveswaran, Praneet Talwar, Zhouran Wang, Sharan Kumar Nagendiran, Aniket jadhav, Prajwal, Bharat, Neeraj, Devesh, Sujit Mayuresh, Raghavender Tummala, Arun Reddy Chitikela.

Table of Contents

List of Figures

List of Tables

Abstract

The usage of aluminum in the automobile industry has been significantly increasing but they have poor tribological properties. The purpose of the study is to develop a low-cost coating using suitable material to increase the wear properties of widely used Aluminum alloys. The material used is the Iron manganese (Fe-Mn) alloy because it's one of the hardest steels and wear resistance is superior to the conventional stainless steels. Fe-Mn alloy is tended to oxidation and depletion of manganese during the conventional spray processes. So, from all the thermal processes cold gas dynamic spray eliminates the oxidation process helping in the deposition of the Fe-Mn alloy.

To improve the efficiency a novel Co-axial laser assisted cold spray process with a dual feed rectangular nozzle has been utilized. The coatings were developed at different laser powers and constant parameters on a 4.5" diameter and 0.5" thick Aluminum 6061 pucks. The influence of laser on the coatings were then investigated using microstructure & phase analysis, micro hardness, wear resistance, and bond strength analysis

Chapter 1: Introduction & Background

Automakers are making significant strides and continue serious ongoing efforts to remove additional weight from the upcoming vehicles. Alternative materials that can replace cast iron will result in significant weight reduction. Substituting iron based alloys with aluminum is one way to achieve weight reduction because of its low density. Many automobile companies have been switching to aluminum constantly. So, far aluminum has been replaced in the components which are not prone to constant wear.
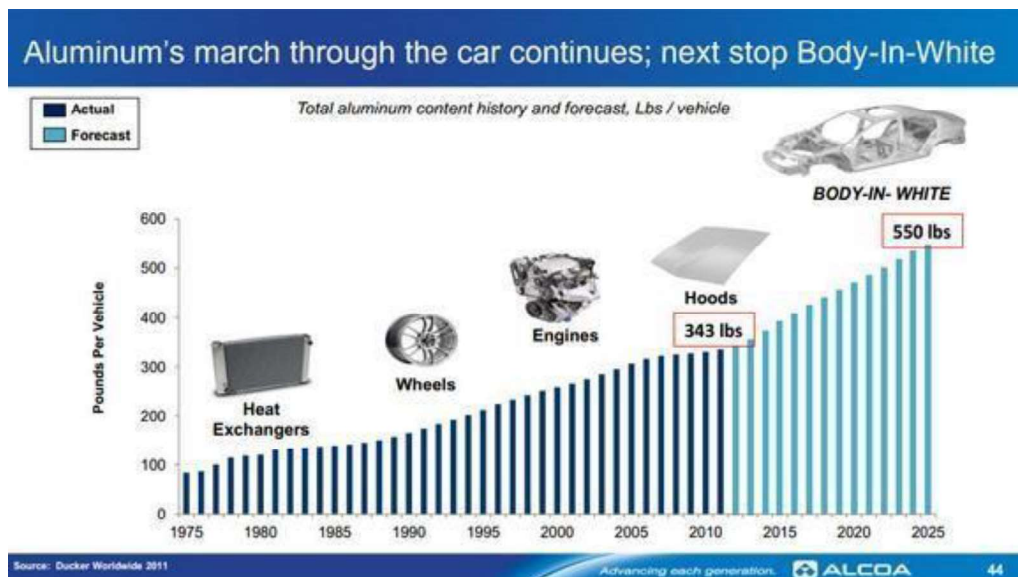
Figure 1.1 Growth of use of aluminum in automobile industry

However, aluminum has poor wear properties and cannot be used in applications where wear resistance is critical. Therefore, a wear resistant coating on the aluminum is necessary for such applications

This study focusses on the development of the low-cost coatings that can improve the wear properties on the most used aluminum alloys. The material used is the Iron manganese (Fe-Mn) alloy because it's one of the hardest steels and wear resistance is superior to the conventional stainless steels. Fe-Mn or the Iron-manganese alloy was discovered in 1888 by Sir Robert Hadfield. It's been gained considerate interest for its properties like high strength and ductility. This material is being gaining interest mainly by the car manufacturers because of its exclusive properties. Multiple deformations are formed which are dependent on the alloy composition and temperature which results in the excellent mechanical properties. High manganese steel alloy such as Hadfeild steel exhibits a combination of properties like high strength, high impact and wear resistance. The mechanical properties vary with the contents of carbon and manganese which makes the tensile strength and ductility decrease as the carbon content is increased. As the level of manganese increase the austenitic phase can be retained and can also work without the presence of nickel. Manganese reduces the corrosion resistance property but the addition of aluminum and chromium influence the improvement on corrosion.

Iron manganese binary(Fe-Mn) and ternary(Fe-Mn-C) alloy has the combination of ductility and strength. The hardening of the material happens because of the manganese present in it by transforming it to the austenic phase. In pure iron the A4(1394°C) and A3(912°C) transformations take place at constant temperatures. Elements like manganese raise the A4 and lower the A3 transformation temperatures which increases the extent of the gamma field in iron carbon phase. Iron manganese binary has become a basis for the new class of metals manufactured by powder metallurgy.
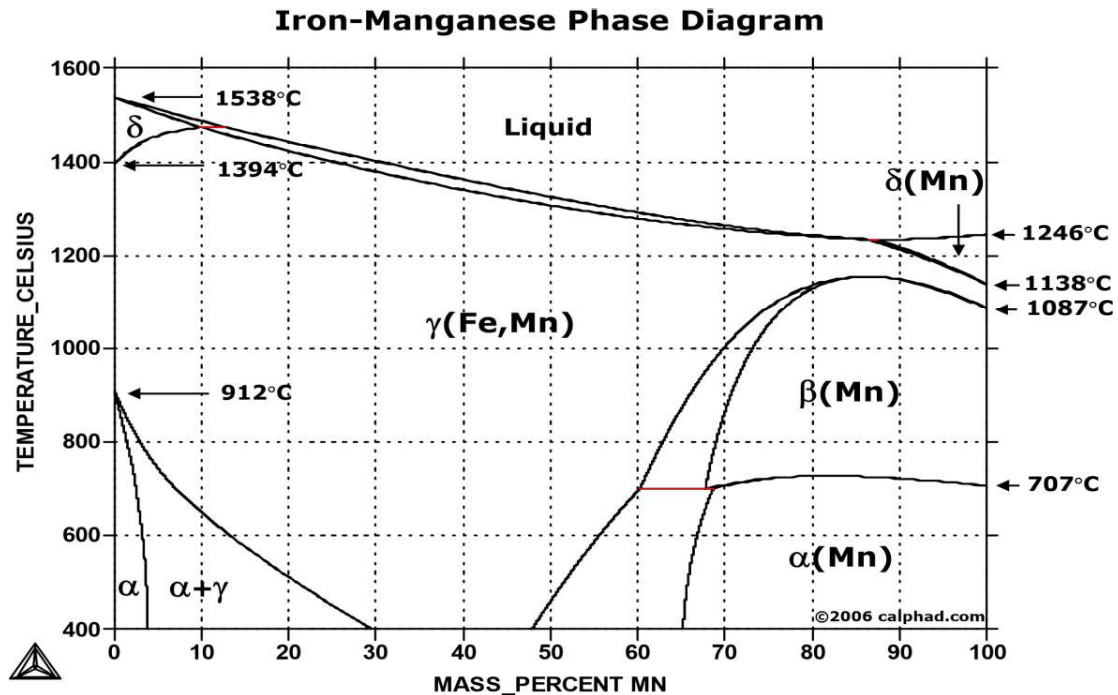
Figure 1.2 Iron-Manganese phase diagram

The phase diagram shows which phases are to be expected at equilibrium for different combinations of manganese content and temperature. The melting point iron and manganese at the pressure of 101325 Pa is 1538°C and 1246°C respectively. Fe-Mn alloy is tended to oxidation and depletion of manganese during the conventional spray processes.

1.1 Background:

1.1.1: Thermal spray

Thermal spray is the term for a group of coatings used to apply metallic or non-metallic coatings. Thermal spray is the process in which a metal or alloy in molten or semi molten to make a layer on a substrate. The particles are accelerated and propelled toward a prepared surface by process gas or atomization jets. Upon the impact bonding is formed with the substrate with the particles causing buildup of thickness and forming a structure. Coating material available for

thermal spraying includes metals, alloys, ceramics, plastics, composites. They are fed in powder or wire form. The advantage of this processes is that huge variety of materials can be used. The disadvantage is that when deposited because of incomplete fillings or wetting of molten metals cracks are formed after the solidification of the molten material. When coatings are done, it results in a phase change and a microstructure with variations in degrees of porosity, solidifications stresses and poor corrosion resistance. Coatings quality is usually assessed by measuring its porosity, oxide content, macro and micro hardness, bond strength and surface roughness. At present thermal spray is being used by many companies as a basic coating development process with good corrosion resistance, wear characteristics and thermal barrier coatings.

1.1.2 Different methods of Thermal spray:

There are different types thermal spray methods available to make coatings to improve surface properties for protection against corrosion and wear. The different types of thermal sprays are:

1.1.2.1 Plasma spraying

1.1.2.2 Detonation spraying

1.1.2.3 Wire arc spraying

1.1.2.4 Flame spraying

1.1.2.5 High Velocity Oxy-Fuel coating spraying (HVOF)

1.1.2.6 High Velocity Air Fuel (HVAF)

1.1.2.7 Warm spraying

1.1.2.8 Cold Spraying

1.1.2.1 Plasma spray:

It's the process of spraying molten or heat softened material onto surface to provide a coating. Material in the form of powder is injected into a very high temperature plasma flame, where it is rapidly heated and accelerated to a high velocity. The plasma spray gun comprises a copper anode and tungsten cathode where both are water cooled. Argon, nitrogen, hydrogen, helium are the gases used as the plasma gas which flows around the cathode and through the anode which is shaped as constricting nozzle. The gas generated is heated up to temperature of $17,540°F$ ($10,000°C$). Then the powder is introduced into the plasma jet where it is melted to the temperatures above and achieves a velocity ranging from 120 to 610 m/sec. the powder is so rapidly heated and accelerated that spray distances can be in order of 25 to 150mm.
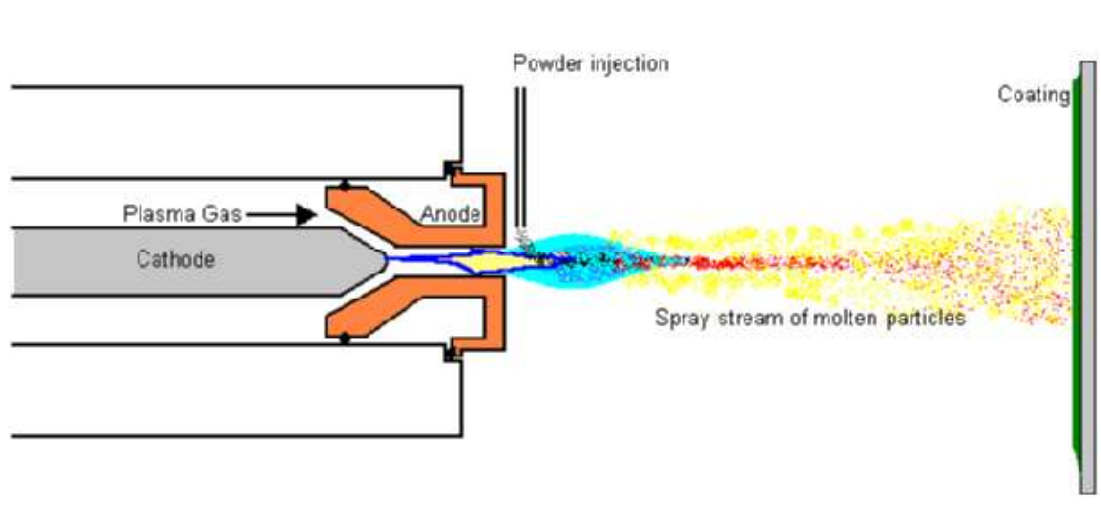
Figure 1.3 Schematic diagram of plasma spray process

Plasma spraying systems can be categorized by several criteria

- Plasma jet generation (direct current, induction plasma)

- Plasma-forming medium (gas, water stabilized plasma, hybrid plasma)

- Vacuum plasma spraying

1.1.2.2 Detonation spraying:

D-gun spray process is a thermal spray coatings process, which gives ab extremely good adhesive strength, low porosity and coating surface with compressive residual stresses. The measured quantity of the combustion mixture consisting of oxygen and acetylene is fed through a tubular barrel closed at one end. To prevent the back firing a blanket of nitrogen gas is allowed cover the gas inlets. The gas mixture inside the chamber is ignited by a spark plug. This ignition of the mixture of gas provides a detonation waves which then propagates through the gas. Depending upon the ratio of the combustion gases the temperatures of the hot gas stream go up to 4000˚C and the velocity of the shock wave can reach up to 3500m/sec. The particles come out of the barrel and impact on the substrate. Depending on the thickness and the type of material for coating material the detonation spraying cycle can be repeated at the rate of 1-10 shots per second.
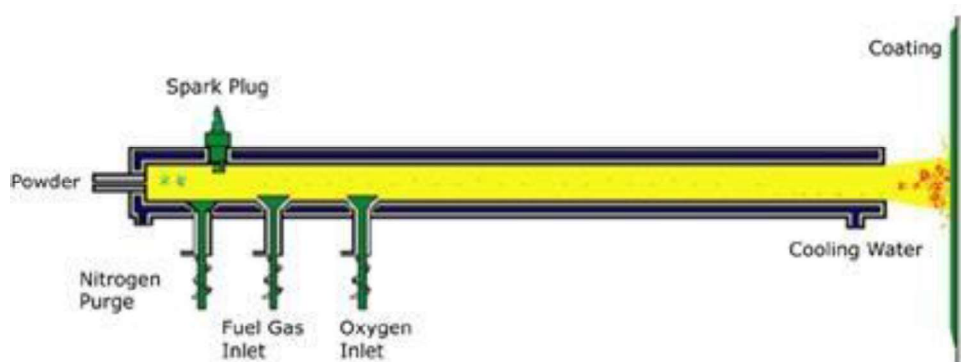
Figure 1.4 Schematic diagram of the Detonation spray process

Once the process is done the chamber is flushed with nitrogen to remove all the hot powder particles from the chamber as these otherwise detonate the explosive mixture in irregular intervals.

1.1.2.3 Wire arc spraying:

Wire arc spray technique is where 2 consumable metal wires are fed independently into the spray gun. The wires are then charged and arc is generated between them. The wires are joined to

make an arc which melts wires and then enters to an air jet from the gun. The molten metal is then deposited onto a substrate. A higher spray rate can be achieved by using a high current rating system like 350A or 700A. the coating formed by this method has relatively high density and adheres well to work piece. High density and bond strength can be achieved by carrying out the process in a reduced pressure chamber. This method is commonly used for metallic, heavy coatings. Anti-corrosion or engineering coatings can be applied by the arc spray. Arc spray system are commonly considered to be easy to operate and to automate. The disadvantage of this process is that only wires that are electrically conductive can be used and if preheating of the work piece is required then a separate source is necessary in this task.
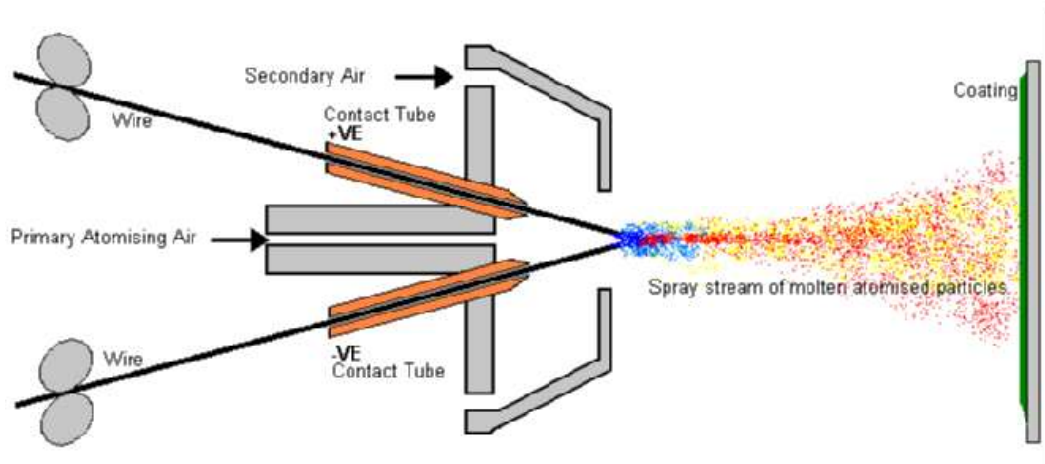
Figure 1.5 Schematic diagram of electric arc spray process

1.1.2.4 Flame spraying:

Flame spray coating is a process in which melted materials are sprayed onto a surface. The feedstock is heated by electrical or chemical means. During the coating process, there is no distortion of the part being coated. The part temperature is generally below 250˚(121˚C) during spray operation. The coating buildup exceed .100in(2.54mm) in thickness, with some   materials

coating can be applied over .200in(5.08mm). The utilization of the flame spraying surface treatment allows the spraying of a wide range of metallic or ceramic coatings on to a large range of component materials where good wear resistance and excellent impact resistance are required.
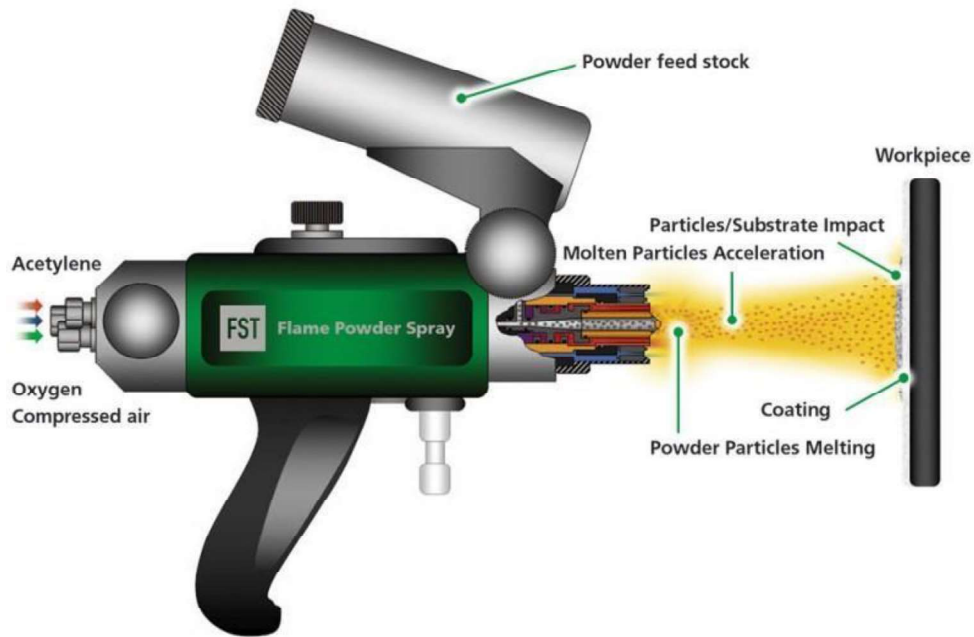
Figure 1.6 Schematic diagram of flame spray process

1.1.2.5 High Velocity Oxy-Fuel coating spray(HVOF):

High velocity Oxy-fuel spraying is a group of thermal spray processes which sprays flames of oxygen and fuels at supersonic speed. The oxygen and fuel are burnt and passed through a nozzle with free expansion which results in supersonic flame gas velocity. Powder particles injected into this gas steam are accelerated to a very high velocity. Fusion is obtained by the kinetic impact of the coating particles rather than by their increased temperature. The temperatures of the particles impacting particles range from 1500 to 2000K. It's difficult to control the temperature of the hot jet and its velocity independently and difficult to optimize the spray parameters because the spraying parameters such as fuel flow rate take time to setup.

8

The advantages of HVOF are that its ideal for coating large components, can produce high-density carbides without degeneration due to high temperature effects and its relatively cold coating process due to brief presence of particles in the hot gas stream.
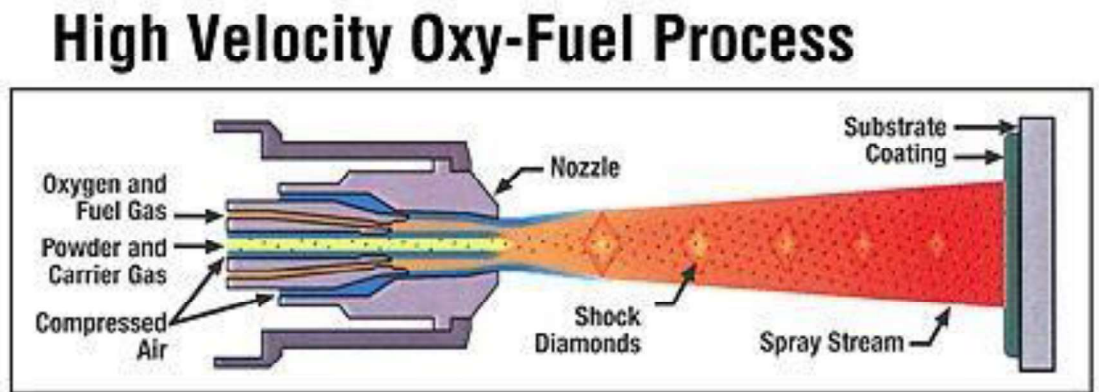
Figure 1.0.7 Schematic diagram of HVOF process

1.1.2.6 High Velocity Air Fuel spraying:

High Velocity Air-Fuel is a thermal spray process for deposition of coatings for protection of parts, vessels and structures against abrasion, erosion and corrosion. HVAF coatings are similar to and generally comparable to coatings produced by HVOF and Cold spray. It's a warm spray but cooler than HVOF but hotter than cold spray. The HVAF process runs on a fuel gas such propane, propylene or natural gas supplied at 140 psi and compressed air supplied by 400 CFM air compressors at 125 psi. Guns utilize axial powder injection into an air-fuel jet with a temperature considerably less oxides than high temperature oxy-fuel jets. HVAF can apply metal, carbide and metal alloy powders of 5 to 53-micron range, with -30+10μm cut being the most common. Deposit efficiency is 50-75% for carbide powders and 60-85% for metal powders.
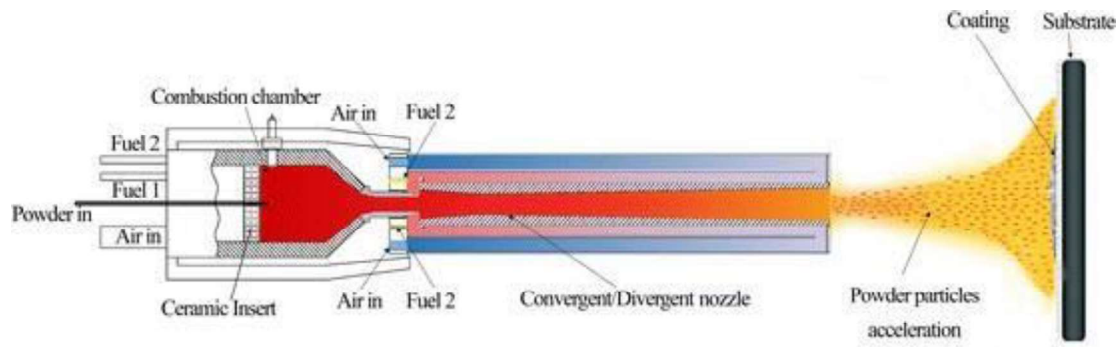
Figure 1.8 Schematic diagram of HVAF process

1.1.2.7 Warm spray:

Warm spray is an atmospheric coating process through continuous impact and deposition of solid particles heated and accelerated by a supersonic jet controlled between 800-1900 K and 900- 1600 m/sec. It's a novel modification of HVOF spray in which the temperature of combustion gas is lowered by mixing nitrogen with combustion gas, thus bringing process closer to cold spraying. The advantages are especially important for such coating materials as Ti, plastics and metallic gases which rapidly oxidize or deteriorate at high temperatures.

1.1.2.8 Cold spray:

Cold gas dynamic spray coating process was discovered in 1980's by a group of Russian scientists performing studies with compressed gas at supersonic velocities. This phenomenon was discovered accidently when the seeding particles formed a coating with extraordinary adhesion. Cold spray is a process where metal powder particles are utilized to form a coating by means of ballistic impingement upon a suitable substrate. The metal powders range in particle size from 5 to 100μm and are accelerated by injection into a high velocity stream of gas. The high-velocity gas stream is generated through the expansion of a pressurized, pre-heated gas through a

converging-diverging nozzle. The velocities are ranged from 400m/s to 1200m/s. The powder particles initially carried by a separate gas stream are injected into the nozzle either prior to the throat or downstream of throat. The particles are then accelerated by the main nozzle gas flow and are impacted onto a substrate after exiting the nozzle. Upon the impact the solid particles deform and create a bond with the substrate. The term cold spray has been used to describe this process due to the relatively low temperatures of the expanded gas stream that exits the nozzle.
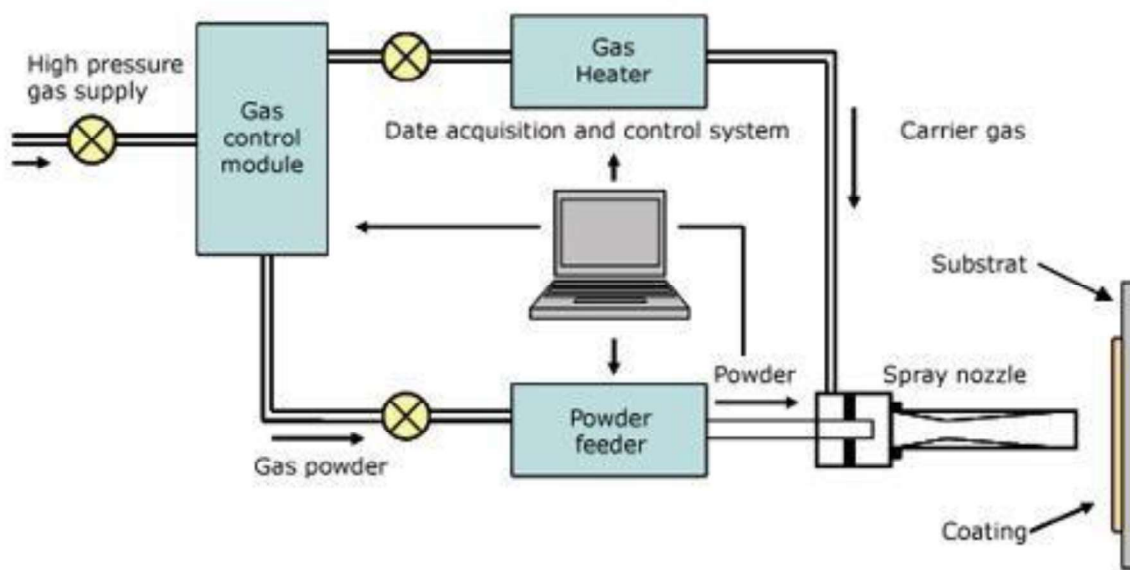
Figure 1.9 Schematic diagram of the cold spray process

By this process the detrimental effects like oxidation, melting of substrate, crystallization, evaporation, stress generation, gas release and other problems which are caused by the high temperatures are reduced. Comparing to the other thermal spray cold spray has the lower temperature working environment.
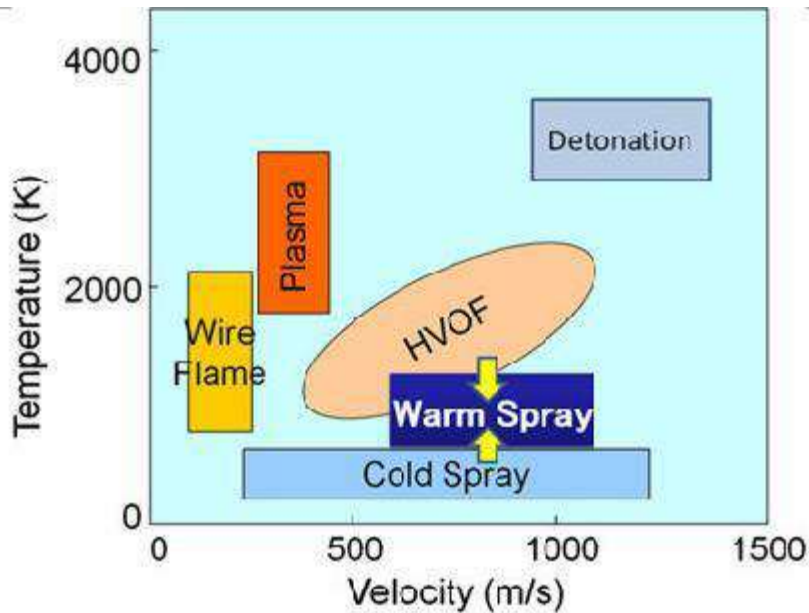
Figure 1.10 comparison of various deposition processes in terms of particle velocity and temperatures

Cold spray system is consisted of high pressure gas tank, powder feeder, gas heater, De laval nozzle and PLC control system. A cold spray system has been buildup in Additive Manufacturing Laboratory which is in University of Michigan-Dearborn. In this system, sprayed particles are feed into the divergent section of nozzle instead of feeding coaxially at convergent section. Cold spray is a parameter sensitive process. The coating quality can be extremely affected by even a slight change in the parameters. So, it is necessary to study effect of process gas conditions, sprayed particle size and substrate temperature which can give a guideline for real experiment and research work. PLC control system most of the experiment parameters can be controlled.

1.2 Advantages, Disadvantages & applications of Cold spray:

Advantages:

- ☐ Low temperature process

- ☐ No combustion fuels and gases are needed

- ☐ Mechanical mixing of particles and substrate like explosive bonding

- ☐ Low oxide and porosity

- ☐ High density deposits

- ☐ Lower energy consumption

- ☐ Minimum surface preparation

- ☐ Short standoff distance

- Possibility to spray micro-sized particles (5-10 µm)

- ☐ Possibility to spray nanomaterials and amorphous materials

Disadvantages:

- Near-zero ductility in the as-sprayed condition.

- Need for ductile substrate

- Difficulty in processing pure ceramics and some alloys as work-hardening alloys

- High cost of helium

- Fouling and erosion of nozzle

Applications:

- ☐ Aerospace- fatigue resistant coatings

- ☐ Chemical- for corrosion resistant

- ☐ Mineral processing

- ☐ Die casting

- ☐ Electronics- creating a heat sink or superconductive surfaces

- ☐ Oil and gas-improved corrosion resistance

- ☐ Glass- platinum coatings

- ☐ Bio-medical- implants

- ☐ Printing-copper coating on rollers

1.3 Cold spray parameters:

Cold spray process mainly depends on its process parameters. The following are the main parameters that influence the coating characteristics:

1.3.1 Gas temperature

1.3.2 Gas pressure

1.3.3 Type of gas

1.3.4 Particle size

1.3.1 Gas temperature:

The gas temperature directly affects the velocity of the particles. The compressed gas enters the convergent divergent nozzle to get the supersonic velocity. The solid powder particles are accelerated by the rapidly expanding gas in the divergent part of the nozzle. In cold spray the main gas is preheated in the heater chamber to the temperature 600˚C. Since the heated gas expands in

the divergent part of the nozzle, the temperature decreases and particles are introduced in this part of the nozzle which makes the temperatures to be lower than the melting temperature of the respective materials.

1.3.2 Gas pressure:

It is known that the particle velocity increases with the increase in the stagnation pressure.

1.3.3 Type of gas:

For cold spray process the type of gas plays an important role in the acceleration of the particles. Generally, nitrogen, helium, compressed air or the mixture of those for main gas or carrier gas because of its lower molecular weights. Initially helium was used but to reduce the cost in the cold spray process nitrogen is being used. But mathematically helium is better than nitrogen because nitrogen has less velocity than of helium and when the temperature of the gas is increased the gas velocity is increased and so the particle velocity.

1.3.4 Particle size:

Particle size plays a prominent role in making of good coatings because the coatings are made by the particles which reach the critical velocity. Particles which are very small cannot make the coatings because they just follow the flow instead of acceleration and very large particles also cannot make the coatings because they cannot get the kinetic energy required form the carrier gas.

Cold spray is chosen from all the thermal processes eliminates the oxidation process helping in the deposition of the Fe-Mn alloy. It's the solid-state approach to deposition and is suitable for the material system that is used. For improving the quality of deposition in the cold

spray a novel co-axial laser assisted process is developed. The studies show that increase in substrate temperature is beneficial for the deposition in cold spray process.

1.4 Co-axial laser assisted cold spray process

Cold spray is the unique solid state deposition process. In this process a high strain plastic deformation helps in binding metal to form a coating. The reviews from the existing literatures confirms that all techniques to improve the efficiency of deposition depends on heating of carrier gas or by increasing the stagnation region in nozzle and increasing the temperature of the substrate for increasing the substrate temperature. In both the cases it is observed that softening the material is the objective. Addition of laser softens the pre-determined amount of precursor. A suitable balance between laser power and particle velocity will ensure successful deposition. In this study the role of laser power is studied. We are using a novel co-axial laser assisted cold spray system unlike the externally aligned laser which is commonly used. The laser beam is passed through the nozzle shaped to fill the inner chamber for the cold spray nozzle.
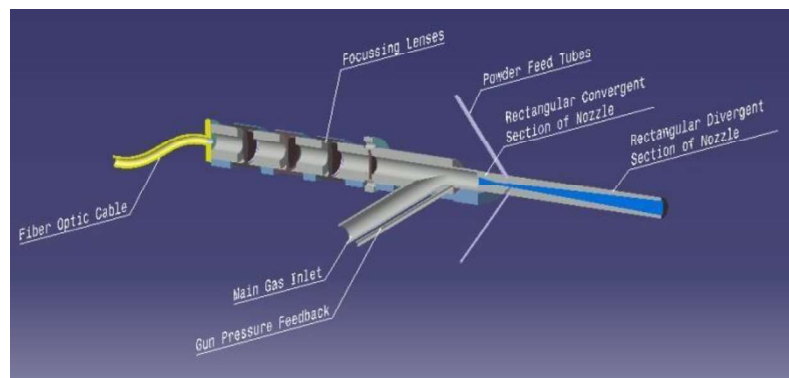

Figure 1.11 The U of M co-axial laser assisted cold spray nozzle

Chapter 2: Cold spray nozzle optimization

2.1 Introduction

In cold spray process the powder particles are accelerated to high velocities using a convergent divergent nozzle. The nozzle geometry to maximize particle velocity is one of the factor in the cold spray. Generally, in present market many nozzles are of round but in this study, we are making a in house rectangular nozzle at Additive Manufacturing Process Laboratory at University of Michigan- Dearborn. The factors we are going to consider are the following:

2.1.1 Injection angle:

The injection angle is the angle for powder injection. The powder can be injected radially or axially. In this study, we are going to design the nozzle in which the powder is injected radially to the throat in the divergent section. The powder velocity is lower than it was axially injected. By doing this we have the advantages of no clogging or wear at the throat and the pressure required for the injection is lower than the stagnation pressure. This allows us to use the low pressure and in-expensive powder feeders.

2.1.2 Expansion ratio:

Expansion ratio is the ratio between exit and throat size of the nozzle. The higher expansion ratio enables gas to accelerate rapidly. The expansion ratio of the nozzle determines the operating regime of the nozzle. Finding a right expansion ratio is very important because small ratios gives

the under expanded flow and the larger ratios give the over expanded flow which results in excessive shock waves and un even flow.

The other factors in the nozzle such as nozzle length and the throat size plays the role in the flow. The expansion ratio is related with the throat size and the length of the nozzle. If the nozzle expansion ratio is related with the throat size and length that may cause the wall friction and decelerate the gas flow.

2.2 Experimental

In this study, we are going to use a house made rectangular nozzle. This nozzle has a conical convergent and rectangular divergent cross-section. Nozzle has a throat of 2.76 mm diameter with an expansion length of 270mm. Nozzle injects particles at 45˚ angle downstream the throat.

Table 2.0.1 Nozzle geometry

Throat Diameter (mm)	Radial injection angle (Degree)	Throat area (mm^2)	Exit area (mm^2)	Exit Aspect ratio	Expansion ratio
2.76	45	5.99	42.89	2.50	7.17
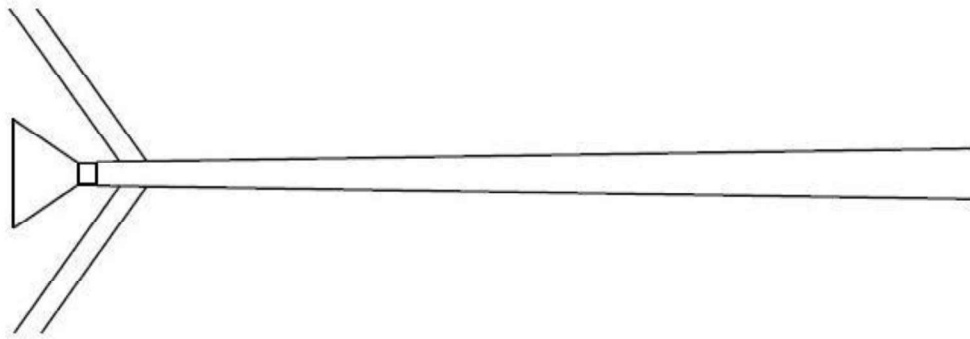
Figure 2.1 Schematic of nozzle with the injection angle 45°

The 3D numerical modeling was performed using ANSYS Fluent. The meshing was done using the workbench meshing tools. The element size was refined based on the area of the nozzle exit. The nozzle inlet was treated at the pressure of 2.7 Mpa and temperature of 873K. A mass flow inlet was introduced to improve convergence. On the front and above the nozzle the pressure was directly applied to the surfaces. The heat transfer between the nozzle walls is not considered. Nitrogen is used at the gas phase by its ideal gas law which takes the compressibility effects into consideration. Discrete phase model was used to inject 15μm particles into the model. The carrier gas flowrate was maintained at 0.002kg/s. the flow rate of particles was set to 0.5g/s under 3% of the flow rate of nozzle gas. Previous studies have used a single feed powder feeder injection port but the nozzle used in this study has a dual powder feeder injection ports.

Figure 2.2 Schematic of the computational flow domain

The mean particle velocity of the nozzle is 599.11± 20.7 m/s.

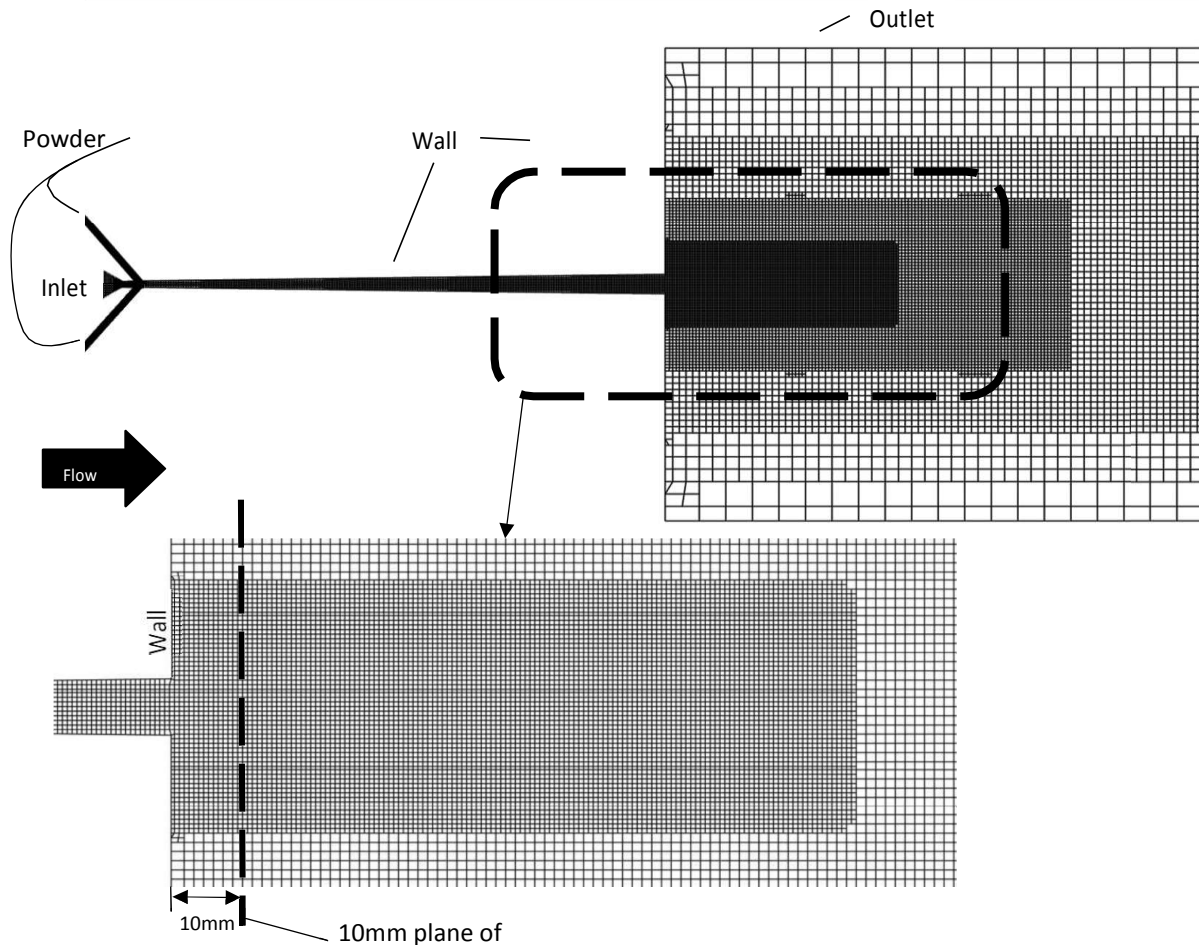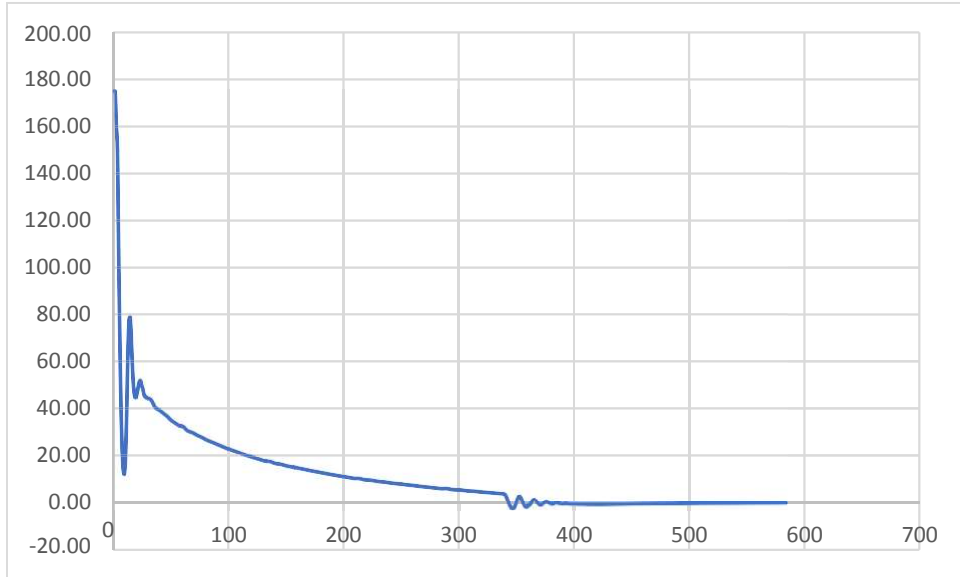Figure 2.3 Static pressure profiles along nozzle axis

The above figure shows that the static pressure in the nozzle along the axial length. The nozzle exit occurs at 0.270m. From this plot, it is evident that the nozzle is operating in under expanded regime

Chapter 3: Experimental setup

The Co-Axial Laser Assisted Cold Spray is conducted at Additive Manufacturing laboratory located in University of Michigan-Dearborn. The system layout is shown below:
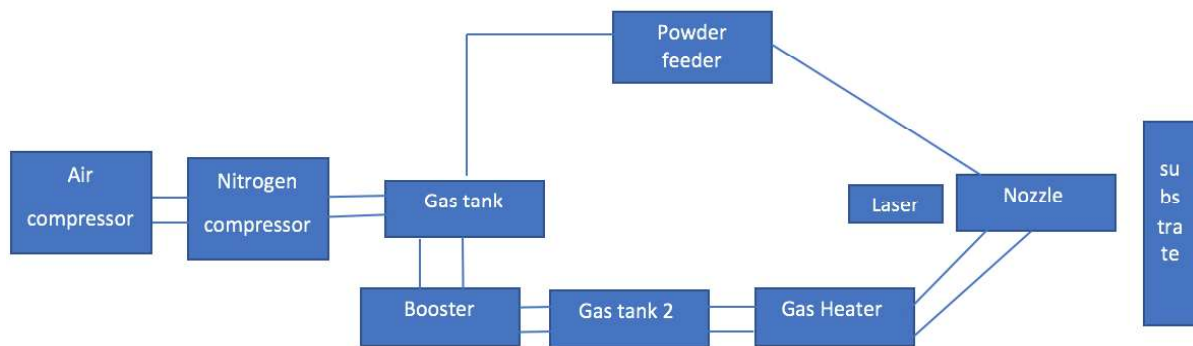
Figure 3.1 Laser assisted cold spray system at AMPL

The advantage of this system it doesn't need external supplier. Nitrogen from the nitrogen generator is stored in the tank which supplies for booster. The booster increases the pressure of the nitrogen to the required. Once it is reached then the nitrogen passes through the heater where it heats up to the required temperature. The pressure and temperature are controlled by PLC. The heated gas is sent to the nozzle and powder feeder sends the powder which is sprayed onto the substrate. The above procedure is for the basic setup. In this study, the hybrid system Co-axial laser assisted cold spray is used. The laser is arranged in such way that the beam can pass co-axially through the nozzle and focusses on the substrate. This study is to observe what difference the laser power makes in weight of coating deposited, change in porosity.

The laser used for the study is a 1KW Trumpf Trudisk 1000 with the 50-micron beam diameter with Gaussian beam profile.
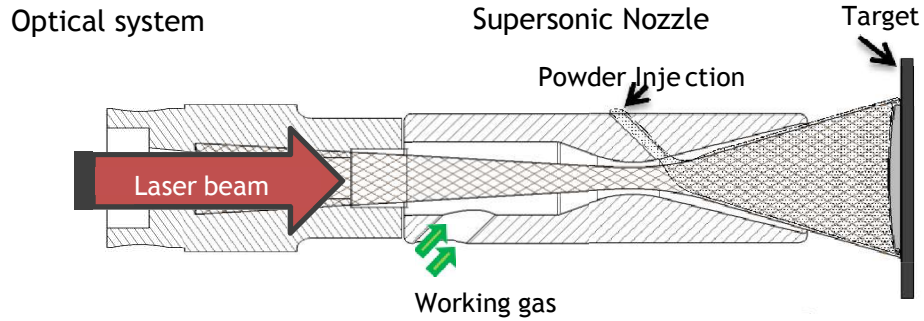
Figure 3.2 Co-axial Laser assisted Cold spray setup

An in-house CNC controller has been built using MACH3 for the rotatory and linear motion during the spray conditions.

3.1 Materials:

Twip is used as the material for the powder stock with a nominal range of 15-45µm supplied by Praxiar Surface technologies (Indianapolis, USA). The particles size distribution was 90%-45µm (-325 mesh).

Table 3.0.1 Composition of Twip powder

Mn	Cr	Al	Fe
35%	4%	2%	Balance
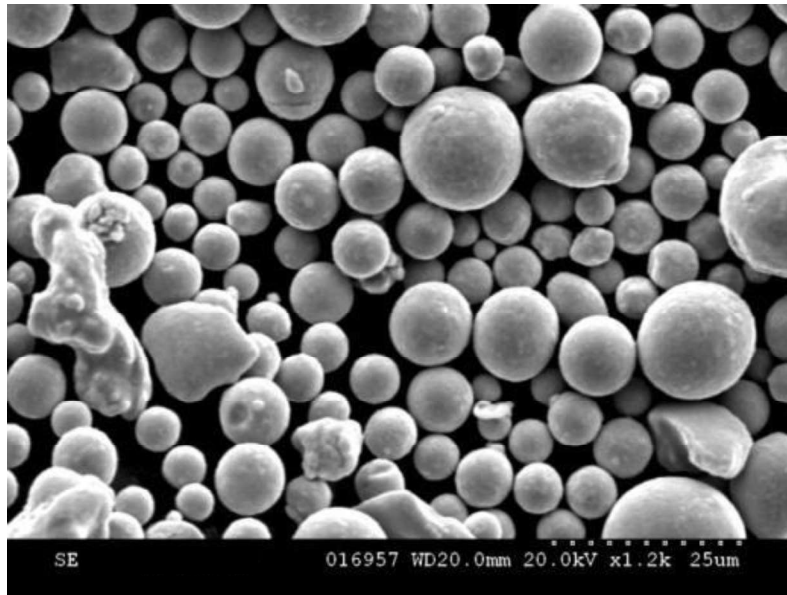
Figure 3.3 SEM of the TWIP powder
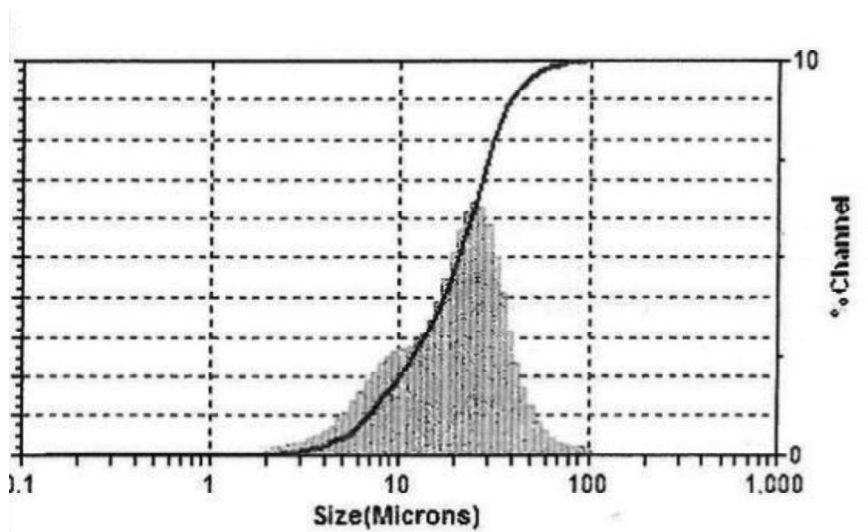
Figure 3.4 Size distribution of the TWIP powder

Substrates used for all the coatings are 4.5" diameter and 0.5" thick pucks of Aluminum 6061. all substrates were made in house with a tolerance of ±0.02" thick.

Figure 3.5 Aluminum puck used for spray

Previous researches has been done on small aluminum samples and never been done on a high scale samples with laser. This study will be focused on the impact of laser on the pucks at different laser power but at a constant CNC speed of 240mm/s.

3.2 Coating parameters:

This research is the study to compare the coating characteristics of twip with different laser powers. The other parameters like gas pressure, feed rate, carrier gas, and CNC speed were kept constant which were decided after a several experiments. Trumpf disk laser is used and parameters are listed below:

Table 3.0.2 Experiment parameters (Set)

Experiment	Main gas pressure (PSI)	Carrier gas pressure (PSI)	Main gas temperature (˚C)	Stand off (mm)	Feed rate (RPM)	Laser power (W)	CNC Speed (mm/sec)
1	500	46	600	10	1.5	0	240
2	500	46	600	10	1.5	100	240
3	500	46	600	10	1.5	200	240
4	500	46	600	10	1.5	300	240

Table 3.0.3 Experiment parameters (Read)

Experiment	Main gas pressure (PSI)	Carrier gas pressure (PSI)	Temperature (˚C)
1	500	46	600
2	500	46	600
3	500	46	600
4	500	46	600

The powder from the powder feeder is sent at a rate of 10g/min. The coatings are sprayed with 1"
wide and 10 layers. The coatings then are cleaned in lathe for the usable thickness. The CNC speed
is calculated with proportional to the diameter and position.

3.3 Characterization of coating microstructure:

The coated samples are then cross-sectioned using EDM cut and mounted in epoxy using
KonductoMet and mounting press supplied by Buehler Company. In this process the epoxy is

melted under high pressure and temperature conditions inside the mounting machine. The sample is then polished to mirror surface finish using 240, 400, 600, 800 and 1200 grit polishing silicon carbide papers using variable speed grinder polisher.

Figure 3.6 Mounting press

Figure 3.7 Polishing machine

The sample is then observed by using Scanning Electronic Microscope(SEM) at a magnification of x150 under SE mode. The SEM used is the Hitachi S-2600N to determine the quality of microstructure of the coatings.

Figure 3.8 SEM

3.4 Phase analysis:

After the initial characterization using SEM for the Phase analysis and crystal structure determination, $X - ray$ diffraction (Rigaku MiniFlex, Cu Kα radiation with $\lambda = 1.5402$ 0A) study was conducted. This test shows whether the material used to spray have underwent any phase change during the coating process.

Figure 3.9 XRD

3.5 Coating micro hardness measurement:

The micro hardness was measured conducted on the sample using micro hardness tester from Struers, Future-tech company at a load of 0.3Kgf for a dwell time of 10 seconds. We measure the hardness using Vickers pyramid number. It is measured by the size of the diamond intend on the sample.

Figure 3.10 Micro hardness tester

15 measurements were conducted on the sample around the coating and then the average of the 15 readings is taken for each sample.

3.6 Coating wear resistance measurement:

The coating wear resistance measurement is conducted in Nano science and engineering lab at University of Michigan- Dearborn. The top surface of the coating is polished until the mirror finish and loaded for wear test. The tribological behavior of the claddings was studied using a CSM ball-on-disc tribometer (CSM Instruments, Switzerland). Dry sliding tests were conducted in ambient air under a load of 5 N and a sliding speed of 35mm/s for a total of 12,000 cycles. Initially both tests were done with stainless steel balls of 6mm diameter. Due to high wear rate of

the ball at room temperature, tests were conducted with tungsten carbide balls of identical

diameter. The weight of the sample and the ball are noted before and after the test.

Figure 3.11 CSM tribometer

The wear track depth measurement is done. We use the stylus type Mitutoyo surface

measurement tester for measuring the depth of the wear track for 7mm.

Figure 3.12 Surface roughness measurement

3.7 Coating Bond strength sample preparation and testing procedure:

Standard ASTM C633 adhesion strength test consist of gluing the cold sprayed samples to grit 24 alumina blasted stainless steel cylinders as bond pins. These bond pins are house made to the dimension of 1.000" diameter. The surface of the bond pin is grit blasted with alumina. The adhesive used is the FM1000 epoxy glue (Cytec Industries, woodland park, NJ) followed by a destructive tensile test which measures the coating-substrate adhesion strength. To ensure proper adhesion between the glue and the metallic surface the samples were heat treated in a furnace.

We have waited for the surface of the bond pin reaches the temperature of 170°C and left it for 3 hours after that. After that they are left to be cooled in at room temperature. 3 Tests on each sample have been done and the average of the 3 tests is presented.

Figure 3.13 Stainless steel Bond pin

Figure 3.14 Bond test setup

Chapter 4: Results and discussions

For TWIP deposition, the Trumpf disk laser is used to heat substrate Co-Axially through the nozzle. The weight measurements, microstructure observation, microhardness, XRD analysis, Wear analysis and bond test are done on the coating areas.

4.1 Coating weight measurement:

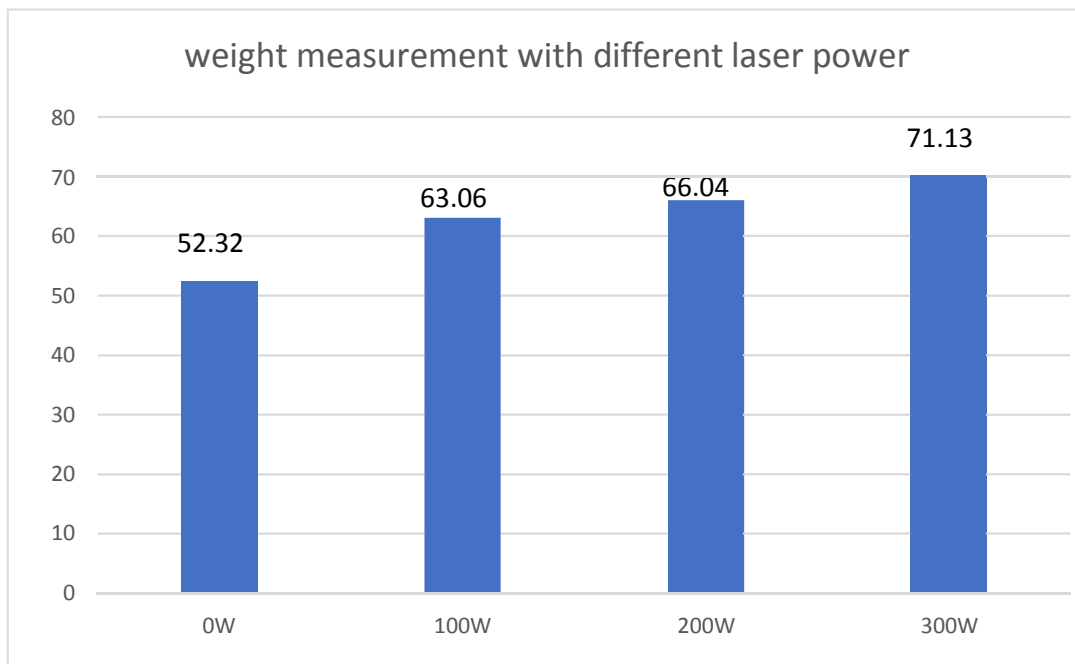The coating weights measured are shown below:

weight measurement with different laser power

Power	Weight
0W	52.32
100W	63.06
200W	66.04
300W	71.13

Figure 4.1 coating weight measurements

(W=Watts)

Table 4.0.4 Coating weight measurement with different laser power

Experiment	Weight before experiment (in gms)	Weight after experiment (in gms)	Total deposition Weight (in gms)
0Watts	332.28	384.6	52.32
100Watts	327.89	390.95	63.06
200Watts	331.03	397.07	66.04
300Watts	332.28	403.35	71.13

From the result, we can see that the maximum coating was observed at 300Watts laser power. We have chosen till 300Watts because above the 300Watts the coating starts to decrease and the coatings starts to pop out. It is known that proper laser treatment can increase the deposition efficiency. This phenomenon shows that as the increase in the temperature on the substrate can keep the temperature at the impact region. The images of the coatings with different laser powers are shown below
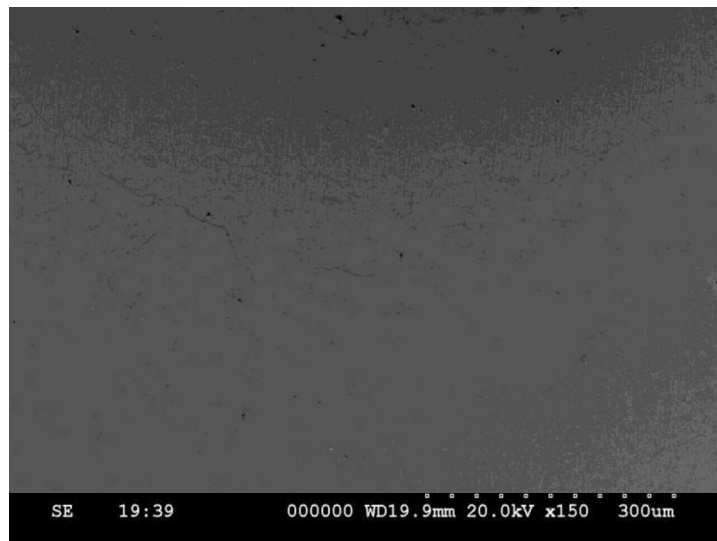
(A)

(B)

(C)

(D)

Figure 4.2 Twip coating pictures (A) 0W (B) 100W (C) 200W (D) 300 W
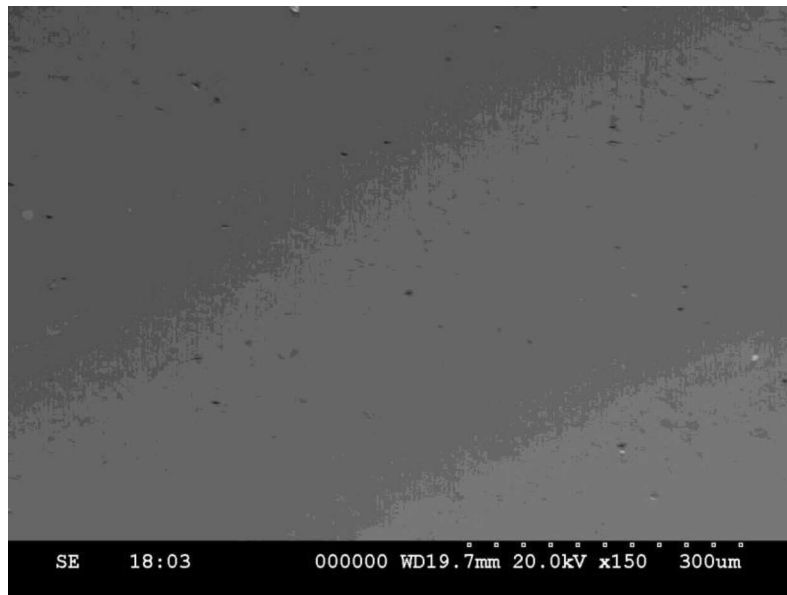
4.2 Coating microstructure:

The microstructure of twip coating with 0Watts, 100Watts, 200Watts, 300Watts laser treatment is shown in the figures below. The pictures are taken at x150 magnification to show the porosity level.

(A)

SE   17:53   000000 WD19.7mm 20.0kV x150   300um

(B)

SE   18:03   000000 WD19.7mm 20.0kV x150   300um

(C)

41
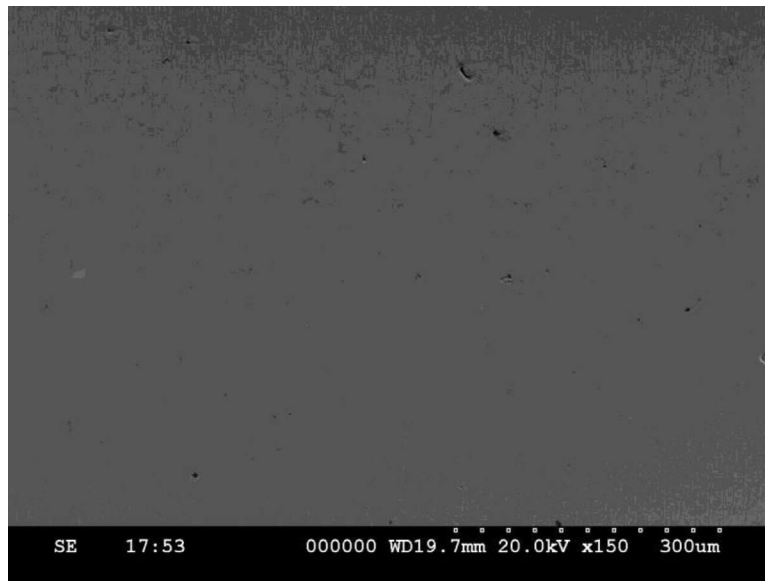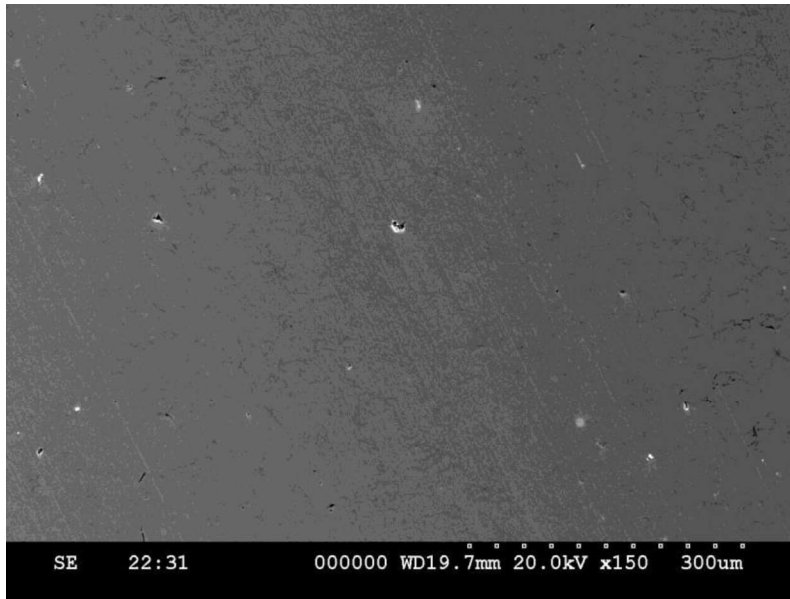
(D)

Figure 4.3 Twip microstructure (A) 0Watts-No laser (B) 100Watts (C) 200Watts (D) 300Watts

To see the microstructure of the coatings we have etched the sample. Etching removes the unprotected layer and shows the microstructure. The etchant we used is the Nitric acid with distilled water. The percentage in the solution made is

Table 4.0.5 Etchant mixture

Name	Percentage
Nitric Acid	5%
Distilled water	95%

The SEM images has been taken at x150 and x300 magnification.

(A)

(B)

(C)

43
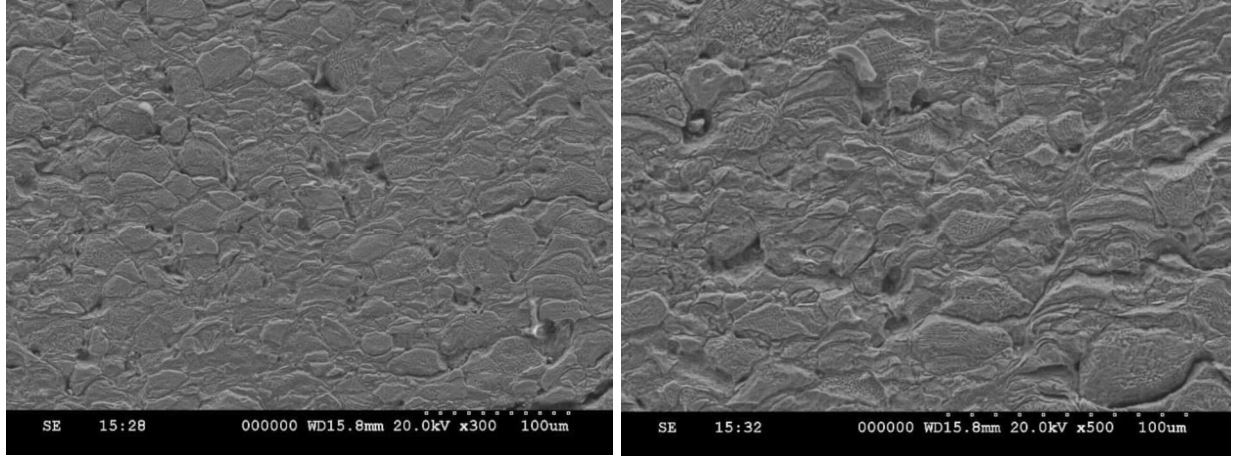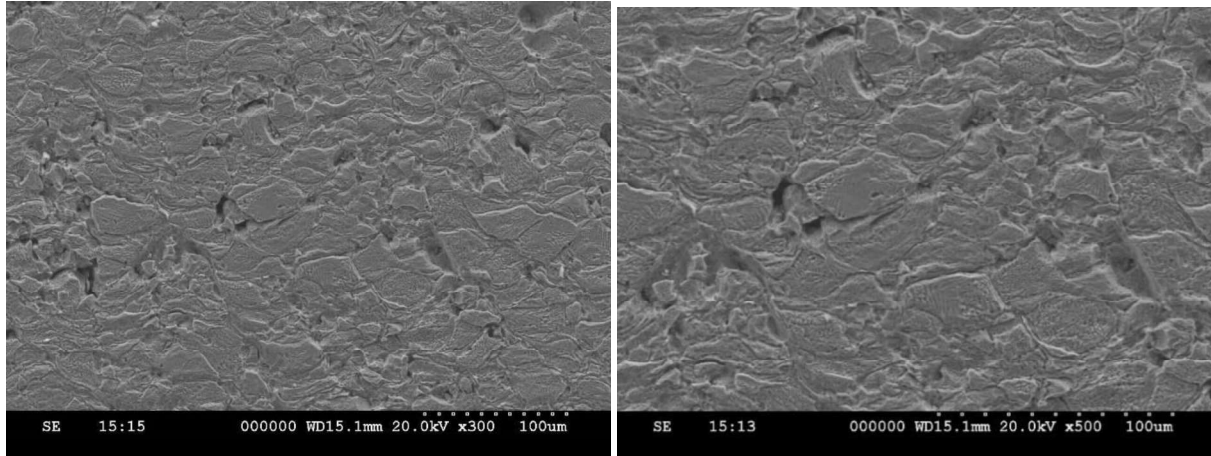
(D)

Figure 4.4 SEM of etched sample (A) 0Watts (B) 100Watts (C) 200Watts (D) 300Watts

From the pictures, we can see that quality of coating with and without laser looks good. But when we look in detail with the non-etched sample we can see the difference between the coatings.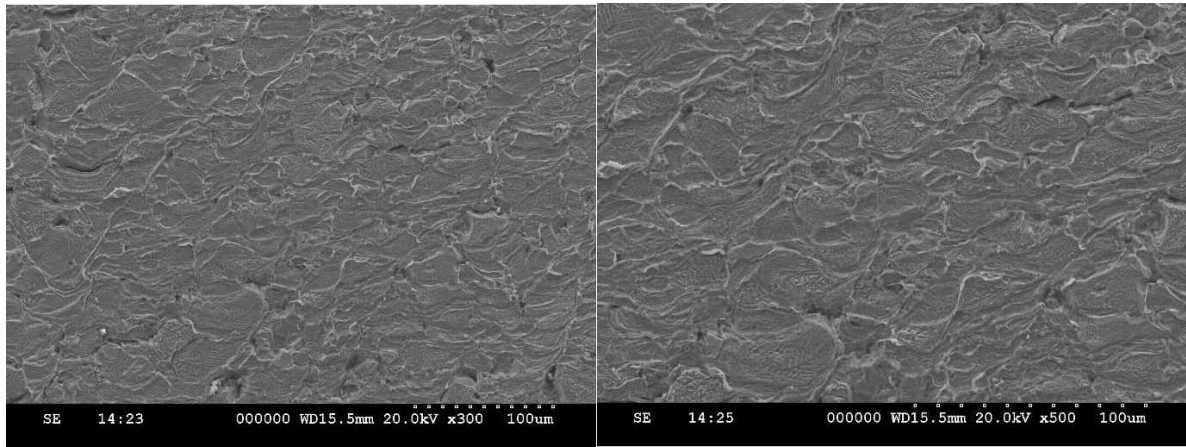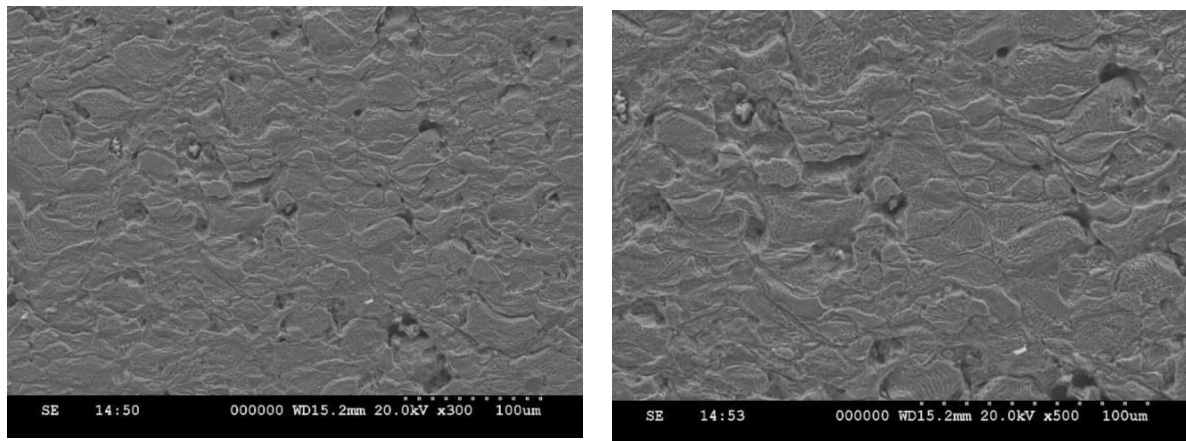 From the pictures, it is observed that quality of coating with and without laser looks good. But when we look in detail with the non-etched sample we can see the difference between the coatings. The SE images of the Cross-sections of the four coatings after etching. The 0Watts coating exhibits poor bonding between particles as show with the arrows. The 100Watts and 200Watts coatings showed an improved layer to layer interface. There are some pits in the 200Watts coating which could have been knocked out during polishing. Although the 300Watts coating is slightly over etched the improvement in compaction and cohesion is similar to 100 and 200Watts coatings.

4.3 Phase analysis:

The phase analysis done by X-ray Diffraction which helps in understanding the phase of the elements in the coating. The advantage of the cold spray is that the temperature is less than the melting temperature of the alloy sprayed so phase change may not be possible but due to the introduction of the laser might affect the phase properties.
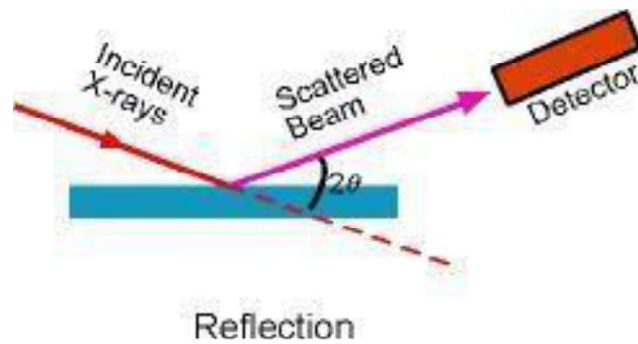
Figure 4.5 XRD principle

The following graphs show the X-ray diffraction of the Twip coatings with the respective laser power.
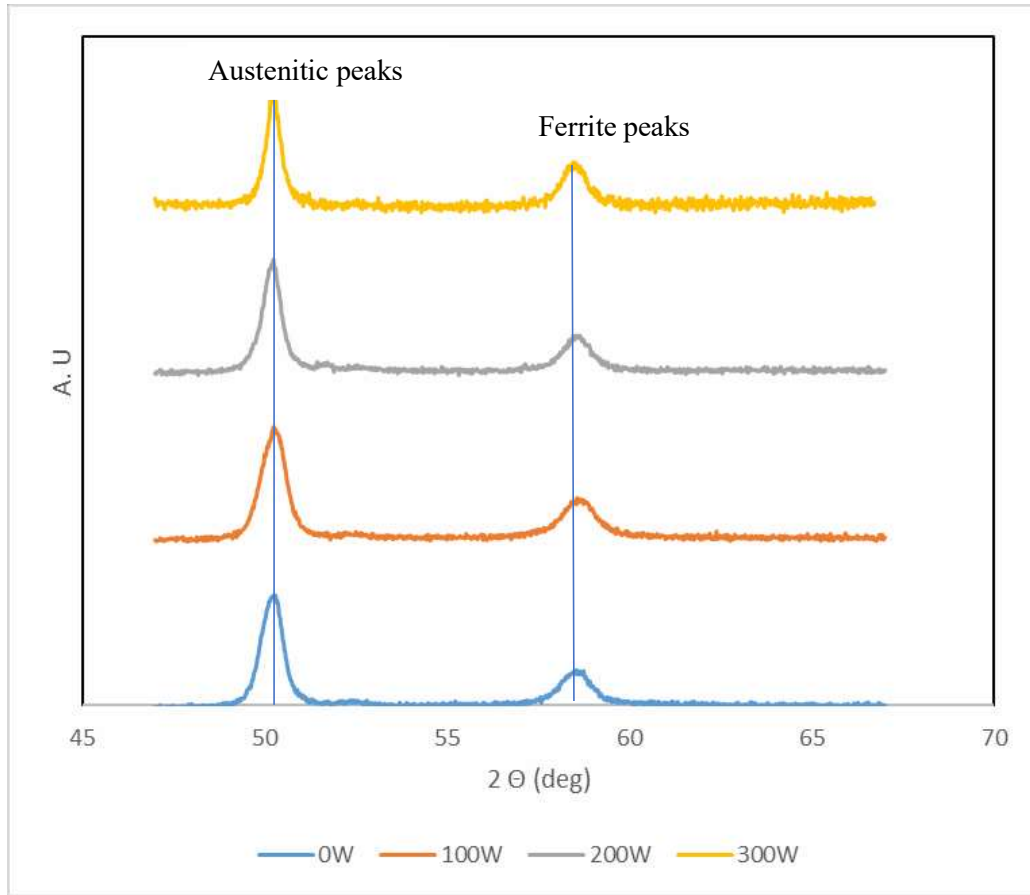
Figure 4.6 XRD plot of TWIP coatings

From the plot, we can see that there is not a big phase change from 0 to 300 W. For twip there was a slight chance of formation of martensitic phase which will be detrimental for coating properties. We have taken JCPDS (Joint Committee on Power Diffraction Standards) to check the austenitic peaks. The JCPDS for the TWIP austenitic peaks is 31-0619.

Due to high temperature and pressure twining of the material the peaks in X-ray diffraction gets split or broadened. Such conditions may also cause micro- stresses and strains. Coatings deposited with the laser showed slight broadening which could be a due to higher stresses that could stem from higher degree of deformation.

CRYSTAL LATTICE   DIFFRACTION LINE

d_0

NO STRAIN

(a)

UNIFORM STRAIN

(b)

NONUNIFORM STRAIN $2\theta \longrightarrow$

(c)
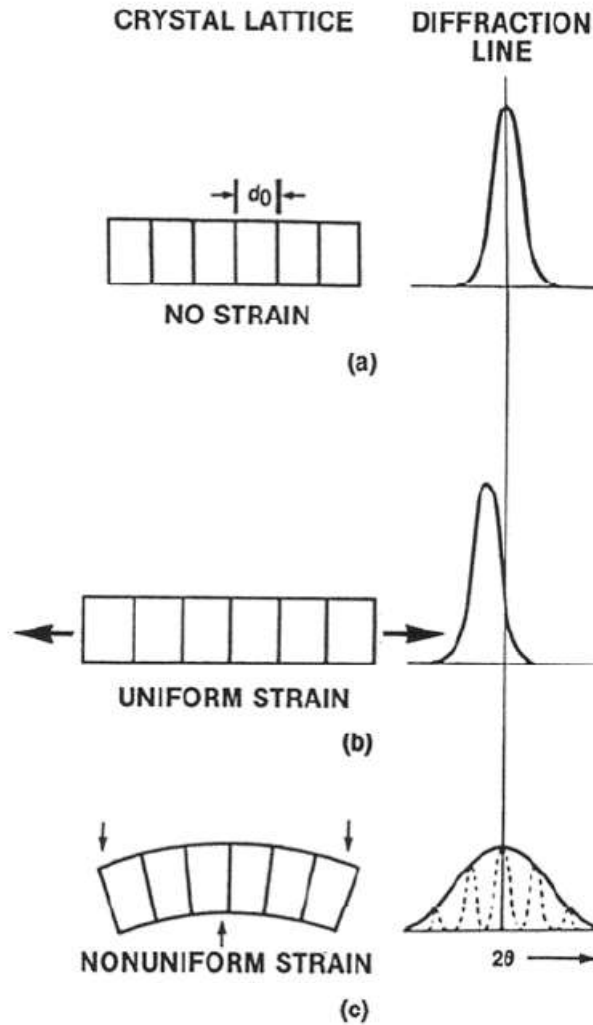
Figure 4.7 Shift and broadening of XRD peaks

4.4 Wear characterization:

To asses coating properties when subjected to sliding friction, wear test is conducted for all the samples. After the wear test the samples weight is taken and the groove depth of the profile is measured with a profilometer. The results are as follows:

Table 4.0.6 TWIP coating weight loss after wear test

Sample	Weight of sample (before) (gms)	Weight of sample (after) (gms)	Weight difference (before) (gms)
0Watts	14.0123	14.0113	0.001
100Watts	14.9486	14.9457	0.0029
200Watts	15.8644	15.8628	0.0016
300Watts	16.3672	16.3662	0.001
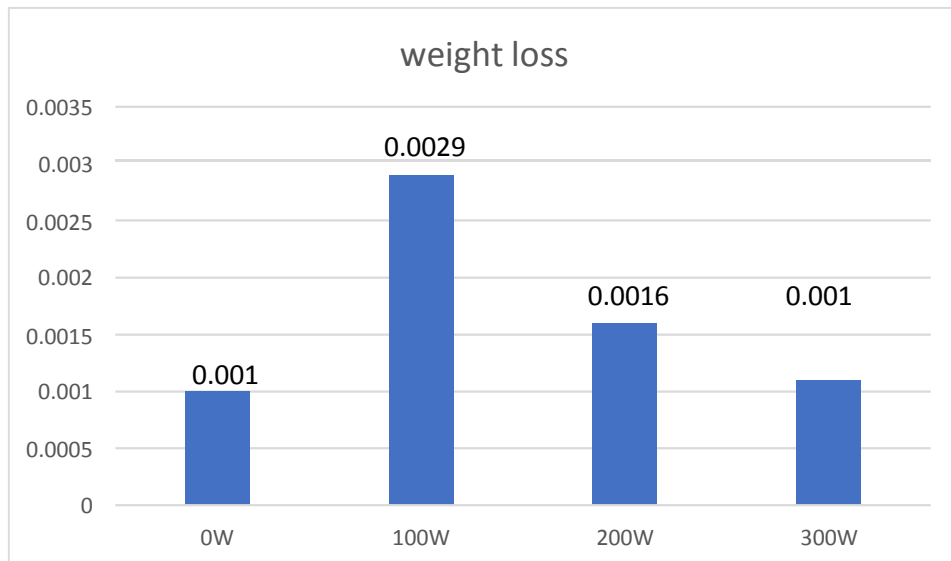
Figure 4.8 Weight loss in the TWIP samples

The following figure shows the wear
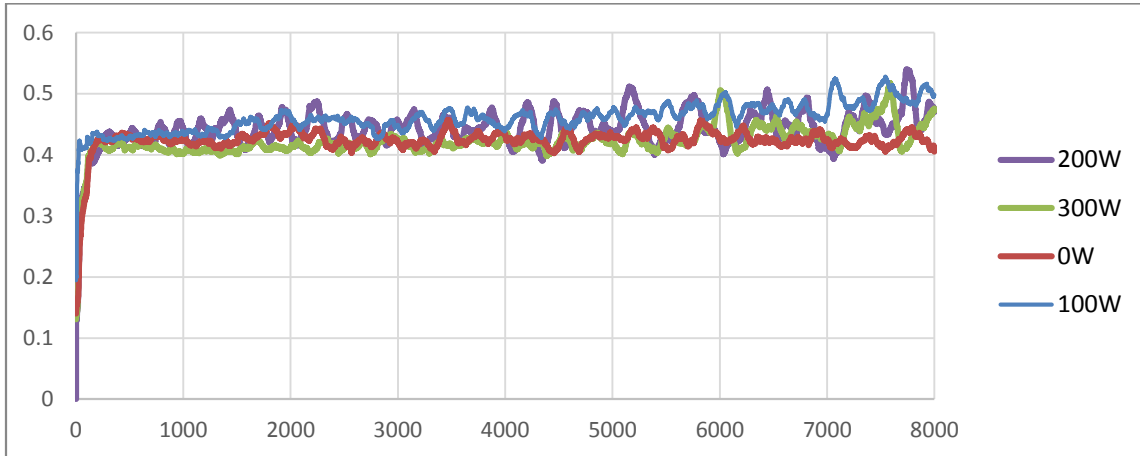
Figure 4.9 Wear test graph (Number of cycles vs coefficient of friction)

From the above results, the coefficient of friction of all the samples are similar.

From the graph the coefficient of friction values can be noted. The following table shows the values from the graph:

Table 4.0.7 Coefficient of friction in wear test

Experiment	Coefficient of friction
0Watts	0.43 ± 0.03
100Watts	0.5 ± 0.03
200Watts	0.47 ± 0.02
300Watts	0.47 ± 0.01

The following graph shows the wear track depth:
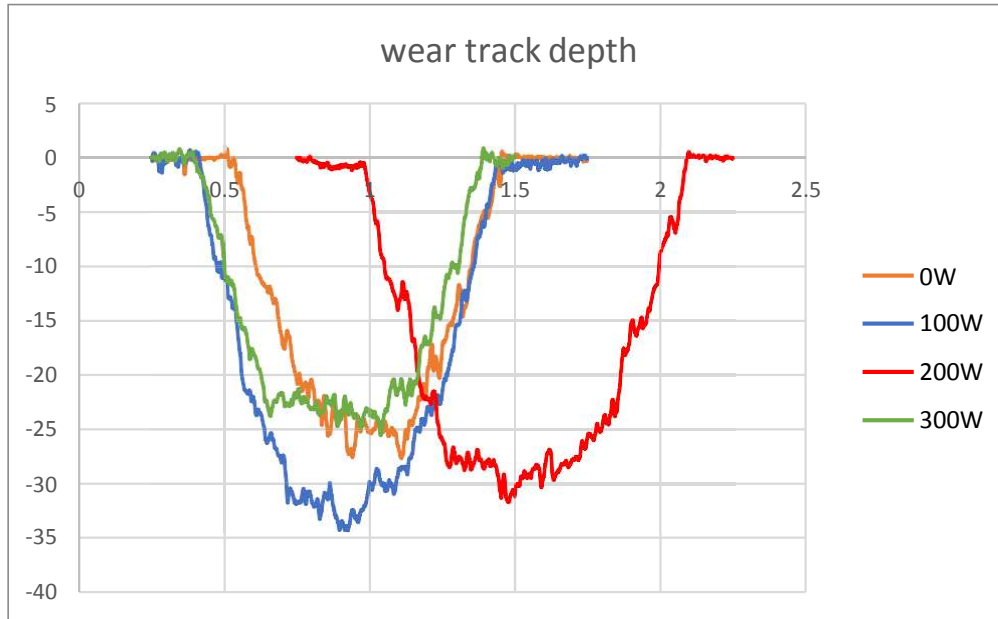
Figure 4.10 Wear track depth

4.5 Hardness measurement:

From the SEM pictures and the deposition weight we have seen that the sample with more laser power has the maximum deposition weight. To check the hardness, we have measured the cross-sectional hardness value. The hardness values are taken at 3 different locations and 4 values at each location. Average of all the points are taken and presented. The following image shows the areas of the hardness values taken:
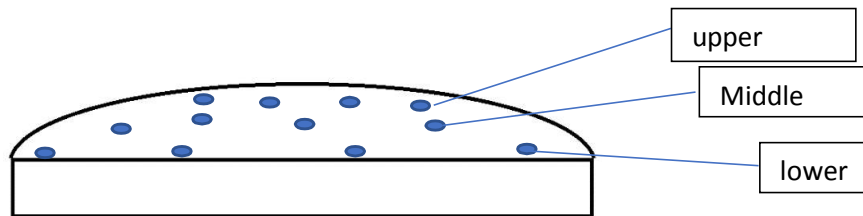
Figure 4.11 Hardness value positions

The average value is given is given in the following table:

Table 4.0.8 Hardness values measured in Vickers

Experiment	Upper (Coating top surface)	Middle (coating)	Lower (Bond line)
0Watts	311± 9	267±61	275±42
100Watts	332±32	266±50	329±29
200Watts	341±29	283±46	342±52
300Watts	301±59	355±80	331±17
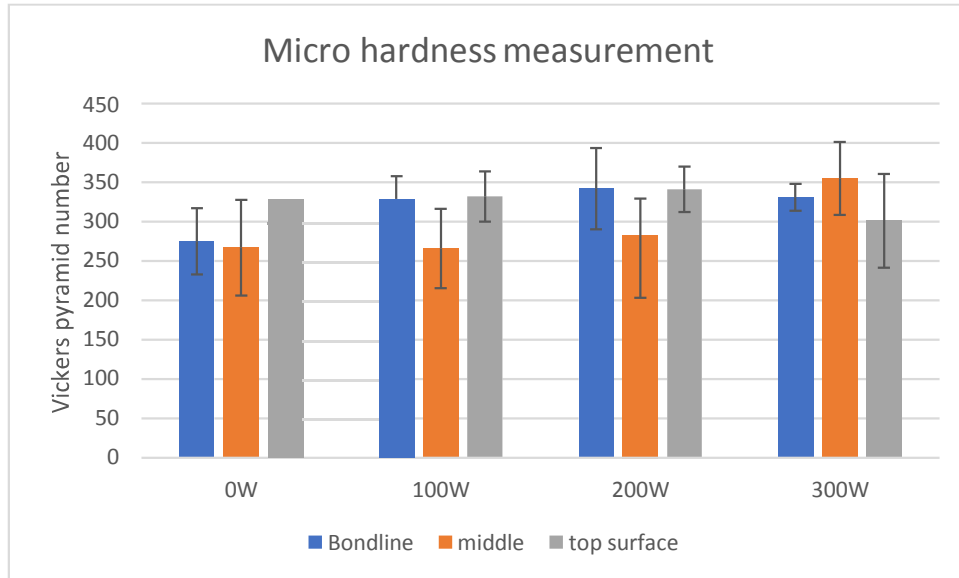
Figure 4.12 Micro hardness values graph

The hardness value at the bond line is increasing with the increase in the laser power it is because of the higher compaction and hence cold worked. the softening can be observed the middle area because of the cold spray gas resulting in the annealing effect. From the overall results, it is observed that the increase in the laser power results in higher coating hardness.

4.6 Coating bonding strength measurement:

Coating bonding strength measurement is conducted on TWIP coatings from 0Watts-300Watts. For the equal heat distribution and the force used on bond pin for proper adhesion are kept equal. The samples are attached to the aluminum plate using a nut and bolt with washer as shown in figure 4.13. 3 readings were taken on each sample and the average value is taken to determine the bonding strength of the coating with the substrate.

From the results, we can see that the bonding strength has been increased with the introducing of the laser. The heating of the substrate has increased the bond between the substrate and the material that is being coated. Without the laser the bond strength is about 27.46

52

Mpa but with the laser it has increased at 7 Mpa to 9 Mpa when the laser is introduced and laser power is increased.

Figure 4.13 Bond testing arrangement

Table 4.0.9 Coating bond strength measurement

Experiment	Bond strength (MPa)
0Watts	27.46
100Watts	34.13

200Watts	35.46
300Watts	32.4

4.7: Coating usable thickness:

The coatings were sprayed till 1.5mm thickness. The application of the coating to be used at the place where there is a friction and light weight is required in the automotive industry. The coatings are cleaned on lathe to see that at what is the thickness of coating that can be left on the sample for the usage after making coating even. The following table shows the usable thickness:

Table 4.10 Coating usable thickness

Experiment	After cleaning (mm)
0Watts	0.5
100Watts	0.67
200Watts	0.75

300Watts	0.95

Its observed that the coatings were cleaned to shiny surface at different thicknesses. The thickness of the coatings for usable purpose has subsequently increased with the increase in the laser power.
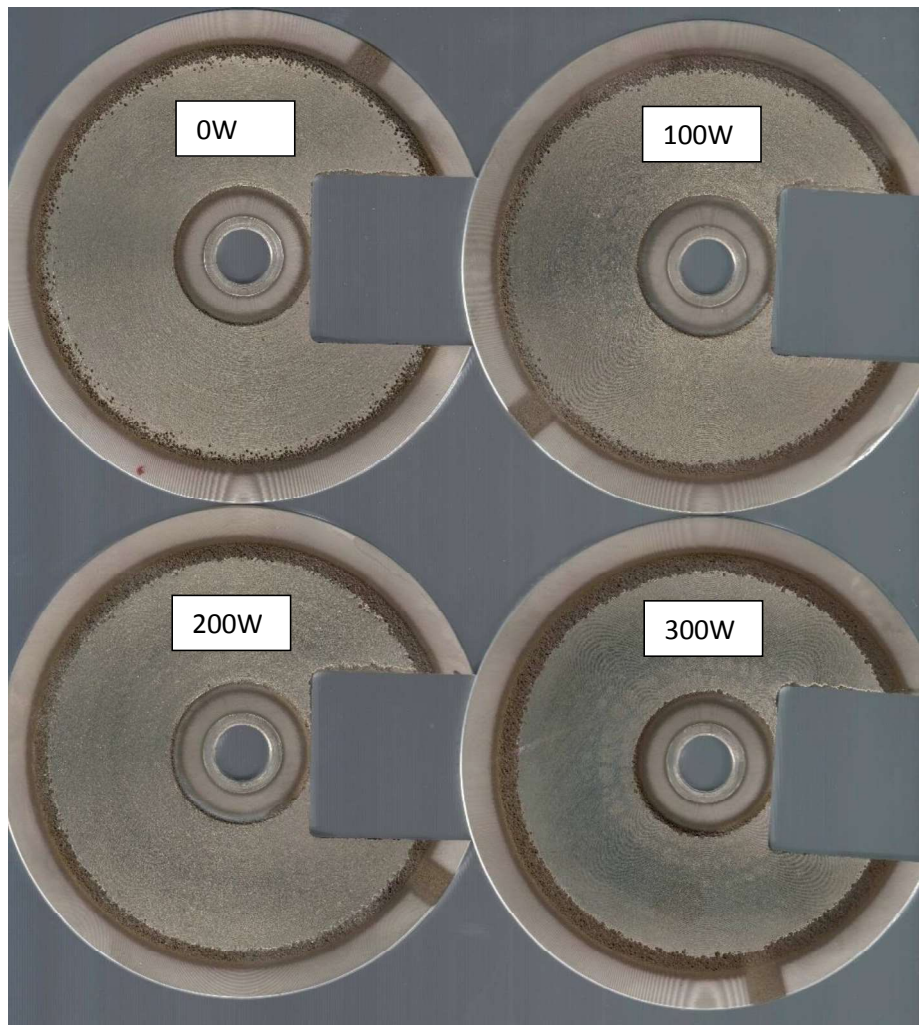
Figure 4.14 Coatings cleaned to usable thickness

The tests done above the 300Watts were not shown because of the decrease in the coating deposition weight and the cracks formed. It can determine that in the Co-axial laser assisted cold spray process the improvement in the deposition is observed with the increase in the laser power up to a limited power density. By increasing the laser power density beyond this limit decrease in the deposition weight and erosion is observed.

Chapter 5: Conclusion

Fe-Mn coatings were successfully deposited with coaxial laser assisted cold spray deposition process. Coating process optimization was carried out at 100, 200 and 300Watts of laser power at a constant surface speed of 240mm/sec. The microstructural images show that the bonding between the layers has been improved with the increase of the laser power. From the XRD analysis it was ascertained that laser did not result in any phase changes in the coating. Wear test, micro hardness and bond test were also performed to determine the coating quality. From all the tests, it was seen that that the strength, deposition efficiency has been increased with the increase in the laser power. Wear test and micro hardness values shows that increase in the laser power has increased the hardness of the coatings. Co-axial laser assisted process showed overall coating quality improvement resulting in thicker coatings with higher hardness and bond strength.

Chapter 6: Future study

. The future study would be to see that what the different laser power does with the different CNC speeds and once the exact speed, laser power is determined the experiment can be carried out at the larger scale so that the can be used in the automotive industry. Further studies are needed to substantiate what laser power does when the dimensions of the samples that need to be coated. The subsequent test at higher loading might reveal the higher results.

References:

- Champagne, Viktor K. •. "The Cold Spray Materials Deposition Process." The Cold Spray Materials Deposition Process - ScienceDirect. N.p., n.d. Web. 21 Apr. 2017.

- "Computational Thermodynamics." Iron-Manganese (Fe-Mn) Phase Diagram. N.p., n.d. Web. 21 Apr. 2017.

- "Plasma Spray." Wikipedia. Wikimedia Foundation, 18 Apr. 2017. Web. 21 Apr. 2017.

- England, Gordon. "Site Links." Thermal Spray Coatings. N.p., n.d. Web. 21 Apr. 2017.

- "TAFA Plasma Spray." Plasma Spray. N.p., n.d. Web. 21 Apr. 2017.

- Guagliano, Mario. "Cold Spray Coating: Review of Material Systems and Future Perspectives." Surface Engineering. N.p., n.d. Web. 21 Apr. 2017.

- Singh Lakhwinder, Vikas Chawla, and J.s. Grewal. "A Review on Detonation Gun Sprayed Coatings." Journal of Minerals and Materials Characterization and Engineering." N.p., n.d. Web.

- Advanced Coating - Thermal Spraying - Detonation Spray Process. N.p., n.d. Web. 21 Apr. 2017.

- Keith Graham Ford, and Christopher John Scott Guest. ""Process for Plasma Plame Spray Coating in a Sub Atmospheric Pressure Environment." N.p., n.d. Web.

- "Analysis and Optimization of the HVOF Process by Combined Experimental and Numerical Approaches." Analysis and Optimization of the HVOF Process by Combined Experimental and Numerical Approaches." N.p., n.d. Web.

- Hiroshi Katanoda., Seiji Kuroda, Makoto Watanabe, and Jin Kawakita. ""Warm Spraying—a Novel Coating Process Based on High-velocity Impact of Solid Particles." N.p., n.d. Web.

- " Design and Optimization of Rectangular Cold Spray Nozzle: Radial Injection Angle, Expansion Ratio and Traverse Speed."Design and Optimization of Rectangular Cold Spray Nozzle: Radial Injection Angle, Expansion Ratio and Traverse Speed. N.p., n.d. Web. 21 Apr. 2017.

- Advanced Coating - Thermal Spraying - Detonation Spray Process. N.p., n.d. Web. 21 Apr. 2017.

- The Effects of Powder Properties on In-flight Particle Velocity and Deposition Process during Low Pressure Cold Spray Process. N.p., n.d. Web. 21 Apr. 2017.

- Optimal Design of a Cold Spray Nozzle by Numerical Analysis of Particle Velocity and Experimental Validation with 316L Stainless Steel Powder. N.p., n.d. Web. 21 Apr. 2017.

- Mohanty, Pravansu S, and The Regents Of The University Of Michigan. ""Patent US20110300306 - Coaxial Laser Assisted Cold Spray Nozzle." Google Books. N.p., 03 Dec. 2010." N.p., 03 Dec. 2010. Web.

- Sharan Kumar Nagendiran. ""METALLIZATION OF KEVLAR /SPALL LINER USING THERMAL SPRAY TECHNOLOGY." Diss. U of Michigan- Dearborn, n.d. Web.

- C. Coddeta., Wen- Ya Lia, Hanlin Liaoa, Hong-Tao Wangb, Chang-Jiu Lib, and Ga Zhanga. "Optimal Design of a Convergent-barrel Cold Spray Nozzle by Numerical Method." N.p., n.d. Web.

- R. Lupoi, and W. O'Neill. ""Powder Stream Characteristics in Cold Spray Nozzles," Surf. Coatings Technol., Vol. 206, No. 6, Pp. 1069–1076, 2011."" N.p., n.d. Web.

- M. Cnrs, L. C. S. Lacs, D. K. Christoulis, M. Jeandin, E. Irissou, J. Legoux, and W. Knapp. ""Laser-Assisted Cold Spray (LACS)," 2009."" N.p., n.d. Web.

- Kang, Xu. ""An Investigation of Laser Assisted Cold Sprayed Titanium and Its Alloy Coating with Experimental and Numerical Methods." Diss. U of Michigan- Dearborn, n.d. Web.

- Julkaisu-Tampere, Koivuluoto, Heli, Tampereen Teknillinen, and Yliopisto. ""Microstructural Characteristics and Corrosion Properties of Cold- Sprayed Coatings." University of Technology. Publication; 882 (2010)."" N.p., n.d. Web.

- "Influence of Process Conditions in Laser-assisted Low-pressure Cold Spraying." Influence of Process Conditions in Laser-assisted Low-pressure Cold Spraying. N.p., N.d. Web. 30 Mar. 2017." N.p., n.d. Web.

- "Corrosion Characteristics of Cold Gas Spray Coatings of Reinforced Aluminum Deposited onto Carbon Steel." Corrosion Characteristics of Cold Gas Spray Coatings of Reinforced Aluminum Deposited onto Carbon Steel. N.p., N.d. Web. 30 Mar. 2017." N.p., n.d. Web.

- E. J. Lavernia, L. Ajdelsztajn, B. Jodoin, E. Sansoucy, A. Zúñiga, and P. Richer. ""Effect of Particle Size, Morphology, and Hardness on Cold Gas Dynamic Sprayed Aluminum Alloy Coatings," Surf. Coatings Technol., Vol. 201, No. 6, Pp. 3422–3429, Dec. 2006."" N.p., n.d. Web.

- M. Doyoyo, Olakanmi, and E. O. ""Laser-Assisted Cold-Sprayed Corrosion- and Wear- Resistant Coatings: A Review." SpringerLink. Springer US, 11 Apr. 2014." N.p., n.d. Web.

- "Effect of Gas Pressure on Al Coatings by Cold Gas Dynamic Spray." Effect of Gas Pressure on Al Coatings by Cold Gas Dynamic Spray. N.p., N.d." N.p., n.d. Web.

- Deposition Characteristics of Titanium Coating in Cold Spraying. N.p., n.d. Web. 21 Apr. 2017.

- T. J. Roemer., Gilmore, D. L, R. C. Dykhuizen, R. A. Neiser, and M. F. Smith. ""Particle Velocity and Deposition Efficiency in the Cold Spray Process." SpringerLink. Springer- Verlag, N.d. Web. 30 Mar. 2017." N.p., n.d. Web.

- "Surface & Coatings Technology 195 (2005) 272 – 279, and Www.elsevier.com/locate/surfco. Www.elsevier.com/locate/surfcoat Effect of Carrier Gases on Microstructural and Electrochemical Behavior of Cold-sprayed 1100 Aluminum Coating (n.d.): N. Pag." N.p., n.d. Web.

- Chou, Da-Tren, Derrick Wells, Daeho Hong, Boeun Lee, Howard Kuhn, and Prashant N. Kumta. ""Novel Processing of Ironâ"manganese Alloy-based Biomaterials by Inkjet 3-D Printing." Acta Biomaterialia 9.10 (2013): 8593-603. Web." N.p., n.d. Web.